Advancing Long-Horizon Hydrological Forecasting: A Mamba-based Approach with Explainable AI for Generalized Streamflow Prediction

Bekir Z. Demiray[1,2,*], Ibrahim Demir[3,4]

[1] IIHR—Hydroscience and Engineering, University of Iowa, Iowa City, Iowa, USA
[2] Interdisciplinary Graduate Program in Informatics, University of Iowa, Iowa City, Iowa, USA
[3] River-Coastal Science and Engineering, Tulane University, New Orleans, LA, USA
[4] ByWater Institute, Tulane University, New Orleans, LA, USA

* Corresponding Author, Email: bekirzahit-demiray@uiowa.edu

Abstract

Accurate long-horizon streamflow forecasting is crucial for water resource management, but existing models often face efficiency and interpretability challenges. This study comprehensively evaluates the Mamba architecture, which utilizes State Space Models for efficient sequence processing, for 120-hour hourly generalized streamflow prediction across 125 diverse Iowa watersheds using 72-hour historical inputs. Performance was benchmarked against Persistence, LSTM, GRU, Seq2Seq, and Transformer models employing NSE, KGE, Pearson's r, and NRMSE. Results demonstrate that Mamba architecture achieves predictive accuracy comparable to, and in several aspects marginally exceeding, the robust Transformer baseline, with both models significantly outperforming other established methods. Critically, Explainable AI (XAI) using SHAP values provided insights into tested models' decision-making, revealing distinct feature utilization patterns and enhancing model transparency. This research highlights Mamba's potential as an efficient, accurate, and interpretable alternative for advancing operational long-range hydrological forecasting.

Keywords: Rainfall-runoff modeling; deep learning; flood forecasting; mamba; transformers; streamflow forecasting

1. Introduction

The increasing frequency and severity of natural disasters worldwide have heightened the demand for more effective forecasting systems that extend beyond immediate warnings. Studies suggest that climate change is a primary factor contributing to the escalation of extreme weather events, leading to more devastating impacts and affecting larger populations (WMO, 2021; UNESCO, 2023; IPCC, 2023). Among these hazards, flooding remains the most prevalent, resulting in widespread economic losses and significant human casualties (WMO, 2021; Alabbad et al., 2024). Evidence indicates that global warming is intensifying flood occurrences, with shifts in precipitation patterns and extreme weather events exacerbating their magnitude (Davenport et al., 2021; NOAA, 2022; Tabari, 2020; IPCC, 2023).

One of the most effective ways to mitigate flood-related damage is through early and accurate streamflow forecasting, which plays a crucial role in disaster preparedness and water resource management (Alabbad et al., 2023). As climate change drives more frequent and severe hydrological extremes, the need for reliable streamflow predictions has become more pressing (IPCC, 2023). Advanced forecasting models not only enhance early warning systems but also play a fundamental role in various hydrological applications, influencing watershed management, agricultural planning, and climate change adaptation policies (Ng et al., 2023; Eccles et al., 2021; He et al., 2023). Accurate forecasts enable better decision-making in critical areas such as precision agriculture (Tanir et al., 2024) and flood risk assessment (Cikmaz et al., 2025; Ahmed et al., 2021; Yaseen et al., 2018). However, due to the nonlinear and dynamic nature of hydrological processes, achieving high-accuracy predictions remains a persistent challenge (Honorato et al., 2018; Eccles et al., 2021; Jia et al., 2024).

A range of forecasting techniques has been developed over time, broadly categorized into physics-based models and data-driven approaches. Physics-based hydrological models rely on mathematical representations of physical processes governing streamflow generation, such as precipitation-runoff relationships, soil infiltration, evapotranspiration, and groundwater interactions (Sit et al., 2021; Ewing et al., 2022). These models simulate streamflow based on governing equations derived from hydrological principles and watershed characteristics (Beven & Kirkby, 1979; Ren-Jun, 1992; Arnold et al., 1994; Devia et al., 2015). Despite their interpretability and ability to incorporate physical laws, physics-based models face several limitations. They require extensive calibration, rely on high-quality meteorological and hydrological data (Sit et al., 2021), optimized data structures (Demir and Szczepanek, 2017) and often involve significant computational costs (Mosavi et al., 2018; Sharma & Machiwal, 2021). Additionally, their predictive performance tends to degrade over long-term horizons, primarily due to uncertainties in parameter estimation and simplifications of real-world hydrological processes (Liu et al., 2022; Castangia et al., 2023). These challenges have motivated researchers to explore data-driven models, which leverage historical datasets to capture complex, nonlinear relationships in streamflow dynamics.

The growing availability of hydrological datasets and advancements in computational power have fueled the rise of machine learning (ML) and deep learning (DL) approaches for streamflow

forecasting, mirroring their widespread adoption across many scientific and engineering domains (Goodfellow et al., 2016; Sarker, 2021; Reichstein et al., 2019; Mankari and Sanghavi, 2025; Khan et al., 2022;). Unlike physics-based models, data-driven methods do not rely on explicit physical equations; instead, they extract patterns and dependencies directly from historical data (Yaseen et al., 2015). Traditional machine learning techniques, such as Support Vector Machines (SVMs), Random Forests (RFs), and Artificial Neural Networks (ANNs), have been applied to many environmental challenges including streamflow prediction, demonstrating improved efficiency in some cases compared to physics-based models (Granata et al., 2016, Bayar et al., 2009). However, these methods often struggle with long-term dependencies in time-series forecasting and may require extensive feature engineering (Sharma & Machiwal, 2021).

To address these challenges, deep learning models have emerged as state-of-the-art tools for streamflow forecasting. Recurrent Neural Networks (RNNs), particularly Long Short-Term Memory (LSTM) networks and Gated Recurrent Units (GRUs), have gained popularity due to their ability to model sequential dependencies in time-series data (Sit et al., 2022; Ibrahim et al., 2022; Ng et al., 2023). These models have been successfully applied to both short- and long-term streamflow prediction, capturing complex temporal patterns in hydrological data (Kratzert et al., 2018; Zhang et al., 2023; Jhong et al., 2024; Sabzipour et al., 2024). While LSTMs and GRUs were designed to better capture long-term dependencies compared to simpler RNNs, effectively modeling relationships between distant points in extensive sequences can still be challenging due to their step-by-step information flow (Vaswani et al., 2017; Castangia et al., 2023). This motivated the development of architectures that could directly access and integrate information across the entire sequence.

Recent advancements have led to the adoption of Transformer-based architectures in various fields including hydrology, which eliminate the need for sequential processing and leverage self-attention mechanisms to effectively capture both short- and long-range dependencies (Vaswani et al., 2017; Wu et al., 2021; Zhou et al., 2021; Wen et al., 2022; Lin et al., 2022;). Indeed, Transformers have demonstrated strong performance in streamflow forecasting (Liu et al., 2022; Castangia et al., 2023; Demiray et al., 2024; Koya and Roy, 2024; Fang et al., 2024), adapting effectively to varying hydrological conditions and prediction tasks. However, while Transformers improve upon recurrent networks, their self-attention mechanism introduces quadratic complexity, making them computationally expensive and can pose scalability and efficiency considerations in some hydrological applications such as dealing with extensive input sequences in real-time hydrological forecasting (Moreno-Pino et al., 2024; Mucllari et al., 2025; Hou et al., 2025).

Given these computational constraints, new architectures are being explored to maintain the predictive advantages of deep learning while improving efficiency and scalability. One such promising development is the Mamba architecture, based on structured State Space Models (SSMs) combined with a selective mechanism (Gu & Dao, 2023). This design aims to offer an efficient (linear-time complexity) alternative to quadratic-complexity Transformers while demonstrating strong potential for capturing long-range dependencies and achieving competitive

predictive accuracy. However, the application of Mamba models within the hydrological domain, particularly for streamflow forecasting, is still in its early stages. While initial investigations are emerging – for example, Jia et al. (2024) explored a lightweight Mamba variant for daily runoff prediction at three locations – there remains a significant opportunity to evaluate Mamba's effectiveness for more granular, long-horizon hourly streamflow forecasting across a diverse range of catchments.

While deep learning offers high predictive accuracy, their complex internal workings often lead them to function as 'black boxes,' making it challenging to understand precisely how inputs are mapped to outputs. In critical fields such as hydrology and water resource management, this lack of transparency can hinder model adoption, debugging, and the generation of trustworthy, actionable insights. Understanding how a model predicts a certain streamflow value is often as important as the prediction itself for informed decision-making. Consequently, the field of Explainable AI (XAI) has gained significant traction, providing methodologies to interpret complex model behavior. Among these, techniques like SHapley Additive exPlanations (SHAP) values, based on cooperative game theory, have emerged as a robust method for quantifying the contribution of each input feature to a model's specific prediction (Lundberg & Lee, 2017). Integrating such XAI approaches with advanced forecasting models like Mamba is essential for leveraging their predictive power responsibly and effectively in real-world hydrological applications.

Therefore, this study aims to bridge these gaps by providing a comprehensive evaluation of the Mamba architecture for generalized hourly streamflow prediction for the next 120-hours across 125 diverse watersheds in Iowa. We compared model's performance against established baseline models, including Persistence, LSTM, GRU, and the Transformer. Critically, leveraging XAI, specifically SHAP analysis, we aim to interpret the tested models' predictions, shedding light on its feature importance and temporal dynamics in the context of hydrological forecasting.

The remainder of this paper is organized as follows: Section 2 describes the study area, dataset, and preprocessing steps. Section 3 details the predictive forecasting models evaluated, including the Mamba architecture along with baseline methods such as Persistence, LSTM, GRU, and Transformer. Section 4 presents the comparative performance results, introduces the Explainable AI approach used for model interpretation, and discusses the findings derived from both the forecasting experiments and the XAI analysis. Finally, Section 5 concludes the paper and outlines potential avenues for future research.

2. Case Study and Dataset

This research utilizes the WaterBench-Iowa dataset, a large-scale benchmark resource meticulously compiled for data-driven streamflow forecasting research (Demir et al., 2022). Adhering to FAIR (Findability, Accessibility, Interoperability, and Reuse) data principles, this dataset covers 125 distinct U.S. Geological Survey (USGS) gauge locations representing watersheds in various scales across the State of Iowa, USA. The geographical distribution of these locations is illustrated in Figure 1. Data within WaterBench-Iowa was aggregated from

various authoritative sources, including NASA, NOAA, USGS, and the Iowa Flood Center, spanning the period from October 2011 through September 2018.

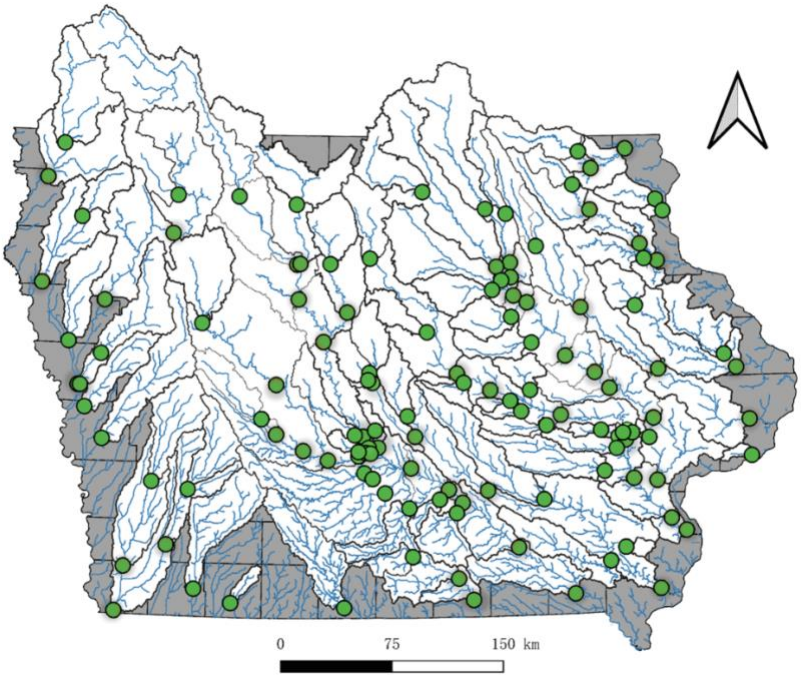

Figure 1. Location of sensor locations (watershed outlets) in Iowa, US (adapted from Demir et al., 2022)

The dataset provides high-resolution (hourly) time-series data essential for hydrological modeling, such as observed streamflow, precipitation estimates, and potential evapotranspiration. Alongside these dynamic variables, it includes crucial static attributes for each watershed, encompassing characteristics like drainage area, average slope, and soil type distributions. This combination of temporal data and spatial attributes, structured conveniently for machine learning applications, facilitates the investigation of hydrological processes under diverse conditions. Key statistics summarizing the watershed characteristics and the hydro-meteorological variables for the study sites are presented in Table 1 and Table 2.

Table 1. Statistical summary of watershed characteristics for 125 USGS gauges in Iowa

	Area (km^2)	**Concentration time (h)**	**Slope**	**Loam**	**Silt**	**Sandy clay loam**	**Silty clay loam**
Min	6	2	0.38%	0%	0%	0%	0%
Max	36,453	315	4.32%	98%	100%	84%	93%
Mean	5,405	77	1.97%	33%	31%	18%	18%
Median	1,918	53	1.80%	33%	21%	4%	7%
SD	8,320	68	0.80%	28%	30%	24%	23%

Table 2. Summary statistics of precipitation and streamflow across 125 watersheds from water year 2012–2018, including missing data analysis

	Annual total precipitation (mm)	**Max. hourly precipitation (mm)**	**Annual mean streamflow (m3/s)**	**Missing rate of precipitation (raw data)**	**Missing rate of streamflow (raw data)**
Min	794	9.1	3	0.02%	0.69%
Max	1,056	60.0	12,963	0.04%	33.14%
Mean	952	24.8	1,926	0.02%	15.16%
Median	961	22.2	608	0.02%	16.14%
SD	57	10.3	2,864	0.01%	6.4%

For developing and evaluating the forecasting models, the dataset was partitioned based on water years. The data from October 2011 to September 2017 constituted the training set, while the final water year (October 2017 – September 2018) was reserved as the independent test set. A validation subset, comprising 15% of the training data, was used for tasks such as hyperparameter optimization and determining early stopping criteria during model training. The data preprocessing steps applied in this work replicate those detailed in the original WaterBench-Iowa publication (Demir et al., 2022) to ensure consistency and allow for direct comparison with established benchmark performances. Lastly, this study focuses on developing a generalized forecasting model. This involves training a single model architecture using the combined data streams from all 125 locations, aiming to capture broader hydrological patterns and enhance model applicability across different catchments within the study region.

3. Methods

This research evaluates the performance of the Mamba architecture for 120-hour hourly streamflow prediction and conducts a comparative analysis against several benchmark models. This section elaborates on the methodologies applied, detailing the Mamba model along with the Persistence, LSTM, GRU, Seq2Seq, and Transformer approaches used as baselines.

3.1. Persistence

The Persistence method, also known as the nearest frame approach, serves as a fundamental baseline for evaluating time-series forecast models, including those for streamflow prediction (Krajewski et al., 2021). This method operates on the simple principle that future conditions will closely resemble the most recent observed state; essentially, it assumes 'tomorrow will be the same as today'. The forecast relies solely on the last available observation, projecting it forward unchanged for the required forecast horizon (n). Mathematically (Eq. 1), the prediction ($\hat{Y}$) at a future time $t + n$ is taken as the observed value (Y) at the current time t:

$$\hat{Y}_{t+n} = Y_t \quad \text{Eq. 1}$$

Despite its simplicity, the Persistence model can be notably difficult to outperform, particularly for very short forecast lead times, often considered less than 12 hours in hydrological studies (Demir et al., 2022). In this study, it provides a crucial benchmark against which the performance of more complex deep learning models is measured.

3.2. LSTM and GRU

Standard Recurrent Neural Networks (RNNs), while designed for sequence modeling, often face difficulties in learning patterns over long-time horizons due to the vanishing gradient problem. This limitation hinders their ability to capture long-range dependencies effectively (Hochreiter & Schmidhuber, 1997). Long Short-Term Memory (LSTM) networks were specifically developed to address this issue (Hochreiter & Schmidhuber, 1997). LSTMs incorporate a memory cell and a system of gates – the input gate, forget gate, and output gate – which meticulously regulate the flow of information through the network.

The core idea involves maintaining an internal cell state (c_t) that acts as an information highway. The forget gate (f_t) selectively discards information from the previous cell state (c_{t-1}), preventing memory overload. Concurrently, the input gate (i_t) determines which new information from the current input (x_t) and previous hidden state (h_{t-1}) should be added to the cell state, often via a candidate state ($\widetilde{c_t}$). These mechanisms allow the cell state to be updated by retaining relevant past information and incorporating new, pertinent data. Finally, the output gate (o_t) filters the updated cell state to produce the hidden state (h_t) for the current time step, which is passed forward in the network. These gating operations, typically using sigmoid and tanh activation functions, enable LSTMs to effectively learn which information to store, forget, and output over long sequences, making them well-suited for hydrological time-series forecasting tasks (Feng et al., 2020; Luppichini et al., 2022; Wilbrand et al., 2023; Ma et al., 2024).

As an alternative to LSTM, Gated Recurrent Units (GRUs) were introduced by Cho et al. (2014). GRUs aim to capture long-term dependencies similar to LSTMs but achieve this with a more streamlined architecture. They typically have fewer parameters than LSTMs, which can lead to reduced computational complexity and faster training times, a potentially significant advantage in complex hydrological modeling scenarios (Guo et al., 2020). The GRU architecture simplifies the gating mechanism by using only two gates: an update gate (z_t) and a *reset* gate (r_t). The update gate merges the functions of LSTM's input and *forget* gates, deciding how much information to carry over from the previous state and how much new information to incorporate. The reset gate determines how much of the past information should be disregarded when computing the current state candidate. This structure allows GRUs to effectively manage information flow and memory while maintaining computational efficiency.

Due to their demonstrated ability to model the non-linear and temporal characteristics of hydrological systems, both LSTM and GRU architectures have been widely adopted and

extensively researched for streamflow forecasting applications (Yaseen et al., 2015; Ibrahim et al., 2022; Tripathy et al., 2024).

3.3. Seq2Seq

Included as one of the established benchmark methods in the WaterBench-Iowa dataset publication (Demir et al., 2022), the Sequence-to-Sequence (Seq2Seq) model utilizes an encoder-decoder framework particularly well-suited for multi-step forecasting tasks where input and output sequences may differ in length (Xiang & Demir, 2022).

The core architecture consists of two main components: an encoder and a decoder, typically implemented using recurrent neural networks. In the specific configuration used here as a benchmark, Gated Recurrent Units (GRUs) serve as both the encoder and decoder units (Demir et al., 2022). The encoder processes the input sequence – comprising historical hydro-meteorological data (e.g., the past 72 hours of precipitation, evapotranspiration, and streamflow) – and compresses the information into a fixed-size 'context vector'. This vector aims to capture the essential features and temporal patterns of the input series.

The decoder then utilizes this context vector, along with any available future input data (e.g., forecasted precipitation and evapotranspiration for the prediction horizon), to generate the output sequence step-by-step. It predicts the streamflow for each hour over the 120-hour forecast horizon, often using the prediction from the previous step as input for the current step. The implementation also employs TimeDistributed wrappers around Dense layers to apply the same transformation at each output time step, potentially followed by a final Dense layer to produce the predictions in the desired format. For further details on the specific architecture and implementation hyperparameters used in the benchmark models, please refer to Xiang & Demir (2022) and Demir et al. (2022).

3.4. Transformer

The Transformer architecture, initially introduced for machine translation tasks (Vaswani et al., 2017), marked a significant advancement in sequence modeling and has subsequently been adopted across numerous fields, including natural language processing, computer vision, and time series forecasting (Wu et al., 2021; Zhou et al., 2021; Lin et al., 2022). Its application to hydrological modeling and streamflow prediction is also an active area of research, showing promising results (Liu et al., 2022; Castangia et al., 2023).

Unlike recurrent models that process sequences step-by-step, the Transformer's core strength lies in its self-attention mechanism. This mechanism allows the model to dynamically weigh the influence of different parts of the input sequence when generating a representation for a specific position. It achieves this by calculating compatibility scores between query, key, and value vector representations derived from the input embeddings. This allows the model to directly capture dependencies between sequence elements regardless of their distance, making it powerful for identifying long-range patterns. Transformers typically enhance this capability

using multi-head attention, where multiple attention calculations are performed in parallel with different learned projections.

Since the self-attention mechanism itself doesn't inherently consider the order of the sequence, positional encodings are typically added to the input embeddings to provide the model with information about the position of each element. In the context of this study, the Transformer model serves as a critical deep learning baseline for comparison against the Mamba architecture. The specific architectural configuration, including layer dimensions, number of heads, activation functions, and other hyperparameters, adheres to the implementation detailed in our prior work investigating Transformers for a related generalized streamflow forecasting task (Demiray & Demir, 2024). For a comprehensive description of the baseline Transformer model implementation used herein, readers are referred to that study.

3.5. Mamba

Mamba is a recent architecture designed to address the limitations of both Transformers and traditional Recurrent Neural Networks (RNNs) in modeling long sequences efficiently and effectively (Gu & Dao, 2023). While Transformers excel at capturing long-range dependencies via self-attention, they suffer from quadratic complexity. Conversely, RNNs and traditional linear State Space Models (SSMs) typically scale linearly but often struggle to capture context effectively over very long distances. Mamba aims to combine the strengths of these approaches, achieving linear-time complexity while maintaining strong modeling capabilities through a selective SSM mechanism.

Mamba is built upon the foundation of structured State Space Models (SSMs). An SSM maps an input sequence $u(t)$ (e.g., $u(t) \in R$) to an output sequence $y(t)$ (e.g., $y(t) \in R$) through an intermediate latent state $h(t)$ (e.g., $h(t) \in R^{\mathrm{N}}$). In continuous form, this is often represented by linear Ordinary Differential Equations (ODEs) (Eq. 2a and Eq. 2b):

$$h'(t) = \mathrm{Ah(t)} + \mathrm{B}u(t) \quad \text{Eq. 2a}$$

$$y(t) = Ch(t) \quad \text{Eq. 2b}$$

Here, $\mathrm{A} \in R^{\mathrm{N}x\mathrm{N}}$ is the state matrix, and $\mathrm{B} \in R^{\mathrm{N}x1}$, $\mathrm{C} \in R^{1x\mathrm{N}}$are projection matrices. To be used in deep learning, these continuous dynamics are discretized using a timescale parameter, Δ. A common discretization method transforms Eq. 2 into a linear recurrence:

$$h_k = \overline{\boldsymbol{A}} h_{k-1} + \overline{\boldsymbol{B}} u_k \quad \text{Eq. 3a}$$

$$y_k = \boldsymbol{C} h_k \quad \text{Eq. 3b}$$

where $h_k \in R^N$is the state at step $k, u_k \in R$ is the input, and $y_k \in R$ is the output. The discrete parameters $\overline{\boldsymbol{A}} \in R^{N\times N}$and $\overline{\boldsymbol{B}} \in R^{N\times \mathbb{1}}$ are derived from $\boldsymbol{A}$, $\boldsymbol{B}$, and Δ through a specific discretization rule (e.g., Zero-Order Hold where $\overline{\boldsymbol{A}} = \exp(\Delta \boldsymbol{A})$ and $\overline{\boldsymbol{B}} = (\exp(\Delta \boldsymbol{A}) - \boldsymbol{I})\boldsymbol{A}^{-1}\boldsymbol{B}$). Traditional structured SSMs (like S4, Gu et al., 2021) impose structure on $\boldsymbol{A}$ (e.g., diagonal) and

keep $\overline{\boldsymbol{A}}$, $\overline{\boldsymbol{B}}$, $\boldsymbol{C}$, and Δ fixed (time-invariant), which allows the recurrence in Eq. 3a to be computed efficiently as a global convolution. However, this time-invariance prevents the model from adapting its behavior based on the input content.

Mamba's key innovation is selectivity. It makes the SSM parameters input-dependent, allowing the model to dynamically modulate the sequence transformation based on the current input token u_k. Specifically, the discretization parameter Δ and the projection parameters $\boldsymbol{B}$ and $\boldsymbol{C}$ become functions of the input sequence:

$$\Delta_k = \tau_\Delta\left(\text{Linear}_\Delta(u_k)\right) \quad \text{Eq. 4a}$$

$$\mathbf{B_k} = \text{Linear}_B(u_k) \quad \text{Eq. 4b}$$

$$\boldsymbol{C_k} = \text{Linear}_C(u_k) \quad \text{Eq. 4c}$$

Where τ_Δ applies a transformation like softplus to ensure $\Delta > 0$. The state matrix $\boldsymbol{A}$ is typically kept fixed (e.g., as a diagonal matrix). This input-dependence means the effective discrete parameters $\overline{\boldsymbol{A}_k}$ and $\overline{\boldsymbol{B}_k}$ in Eq. 3a also become functions of the input u_k. Consequently, the model can dynamically control how information propagates through the hidden state (h_k): it can choose to selectively propagate or ignore information from the past state (h_{k-1}) based on the current input (via $\overline{\boldsymbol{A}_k}$) and selectively focus on or filter the current input (via $\overline{\boldsymbol{B}_k}$). This selective mechanism allows Mamba to perform content-based reasoning similar in spirit to the gating mechanisms found in LSTMs and GRUs.

While selectivity breaks the time-invariance needed for efficient convolution, Mamba employs a hardware-aware parallel scan algorithm. This algorithm computes the recurrence (Eq. 3a) efficiently on modern parallel hardware like GPUs, despite its sequential nature. The scan operation allows Mamba to maintain linear scaling during both training and inference, making it significantly more efficient than standard Transformers for long sequences.

Architecturally, this selective SSM mechanism (often termed S6) is typically embedded within a Mamba block. A standard Mamba block often includes input expansion via a linear layer, a convolutional layer, an activation function (e.g., SiLU/Swish), the core S6 layer, and an output projection layer, usually with residual connections (Gu & Dao, 2023). The Mamba model implemented in this study comprised a single such Mamba block configured with architectural parameters including a model dimension (d_{model}) of 128, an SSM state expansion factor (d_{state}) of 4, a block expansion factor (expand) of 2, and a local convolutional width (d_{conv}) of 2.

The deep learning models were implemented using specific frameworks: the Seq2Seq model was developed using Keras, while the Mamba, LSTM, GRU, and Transformer models were implemented using the PyTorch framework. The training procedure, unless specified otherwise by their original benchmark implementations or framework-specific requirements, followed a common setup. Mean Absolute Error (MAE) was employed as the loss function throughout the training phase. The Adam optimizer was used for model parameter updates, with an initial learning rate set to 1×10. A batch size of 512 was utilized. To aid convergence and prevent overfitting, a learning rate scheduling strategy was implemented where the learning rate was

halved if no improvement in validation loss was observed for 10 consecutive epochs. Furthermore, an early stopping criterion was applied, halting the training process if no improvement in validation loss was noted for 20 consecutive epochs.

4. Results

This section presents the results of the comparative evaluation of the Mamba model against baseline methods for 120-hour hourly streamflow forecasting across the 125 study locations. We first detail the performance based on standard evaluation metrics, followed by an analysis using Explainable AI techniques to interpret model behavior. Finally, we discuss the overall findings and their implications.

4.1. Performance Metrics

To quantitatively assess and compare the effectiveness of the different streamflow forecasting models, this study utilizes four standard metrics widely recognized in hydrological modeling: Nash-Sutcliffe Efficiency (NSE), Kling-Gupta Efficiency (KGE), Pearson's correlation coefficient (r), and Normalized Root Mean Square Error (NRMSE). These metrics offer complementary perspectives on model accuracy, reliability, and overall simulation quality, enabling a thorough evaluation (Kratzert et al., 2018; Xiang & Demir, 2021; Liu et al., 2022).

The following definitions apply to the equations below: Y_i is the observed streamflow at time step i, $\widehat{Y}_i$ is the predicted streamflow at time step i, $\bar{Y}$ is the mean of observed streamflow values, $\bar{\widehat{Y}}$ is the mean of predicted streamflow values, σ_Y is the standard deviation of observed values, $\sigma_{\hat{Y}}$ is the standard deviation of predicted values, and N is the total number of considered time steps.

Nash-Sutcliffe Efficiency (NSE): Proposed by Nash and Sutcliffe (1970), NSE is a widely used metric that determines the relative magnitude of the residual variance ('noise') compared to the measured data variance ('information'). It assesses how well the plot of observed versus simulated data fits the 1:1 line. It is calculated as:

$$\mathrm{NSE} = 1 - \frac{\sum_{i=1}^{N}\left(Y_i - \widehat{Y}_i\right)^2}{\sum_{i=1}^{N}(Y_i - \bar{Y})^2} \qquad \text{Eq. 5}$$

NSE values range from $-\infty$ to 1 (perfect fit). An NSE of 0 means the model is only as good as the mean of the observations, while negative values indicate the mean is a better predictor. Values greater than 0.5 are often considered acceptable in hydrological modeling (Arnold et al., 2012; Krause et al., 2005).

Kling-Gupta Efficiency (KGE): KGE was developed to provide a more balanced assessment by decomposing the error into three distinct components: correlation (r), bias ratio ($\beta = \bar{\widehat{Y}}/\bar{Y}$), and variability ratio ($\alpha = \sigma_{\hat{Y}}/\sigma_Y$) (Gupta et al., 2009; Kling et al., 2012). The formula is:

$$\text{KGE} = 1 - \sqrt{(r-1)^2 + (\alpha-1)^2 + (\beta-1)^2} \quad \text{Eq. 6}$$

Like NSE, KGE ranges from $-\infty$ to 1 (ideal fit). It offers diagnostic value by indicating whether model errors stem primarily from poor correlation, bias in the mean, or misrepresentation of variability. Higher positive values indicate better performance.

Pearson's Correlation Coefficient (r): This metric measures the strength and direction of the linear relationship between the observed (y) and predicted ($\hat{Y}$) values. It is calculated as:

$$r = \frac{\sum_{i=1}^{N}(Y_i - \bar{Y})\left(\hat{Y}_i - \bar{\hat{Y}}\right)}{\sqrt{\sum_{i=1}^{N}(Y_i - \bar{Y})^2}\sqrt{\sum_{i=1}^{N}\left(\hat{Y}_i - \bar{\hat{Y}}\right)^2}} \quad \text{Eq. 7}$$

Values range from -1 to +1, where +1 indicates a perfect positive linear correlation. A high positive r suggests the model captures the linear trends in the observed data well.

Normalized Root Mean Square Error (NRMSE): NRMSE provides a measure of the average prediction error relative to the scale of the observed data, facilitating comparisons across different locations or datasets. Normalizing by the mean of the observed data ($\bar{Y}$), it is calculated as:

$$\text{NRMSE} = \frac{\sqrt{\frac{1}{N}\sum_{i=1}^{N}\left(Y_i - \hat{Y}_i\right)^2}}{\bar{Y}} \quad \text{Eq. 8}$$

Lower NRMSE values indicate better predictive accuracy, signifying smaller errors relative to the mean observed streamflow. These four metrics collectively provide a comprehensive framework for evaluating the performance of the streamflow prediction models presented in this study.

4.2. Experimental Results

This section presents the detailed findings from our experiments on 120-hour hourly streamflow forecasting. The primary objective is to evaluate the predictive efficacy of Mamba architecture. We benchmark its performance against the five baseline models detailed in Section 3: Persistence, Long Short-Term Memory (LSTM), Gated Recurrent Unit (GRU), Sequence-to-Sequence (Seq2Seq), and the Transformer model. The comparison utilizes the four key performance metrics defined in Section 4.1: Nash-Sutcliffe Efficiency (NSE), Kling-Gupta Efficiency (KGE), Pearson's r, and Normalized Root Mean Square Error (NRMSE).

A crucial aspect of the experimental setup involved preparing the input data specifically for the deep learning sequence models, namely LSTM, GRU, Transformer, and Mamba. Consistent with the methodology in Demir et al. (2022), the input features for predicting the subsequent 120 hours of streamflow were composed of static location features, historical dynamic data, and forecast dynamic data. The static features included seven time-invariant watershed

characteristics (e.g., area, slope, soil types). Historical dynamic data encompassed three variables: observed hourly precipitation, evapotranspiration, and discharge from the 72 hours preceding the forecast start time. Forecast dynamic data consisted of two variables: predicted hourly precipitation and evapotranspiration for the 120-hour prediction window.

For models requiring sequence inputs, these components were structured into segments. The historical data, combined with the seven static features, formed an input segment with a total of ten features and dimensions [batch size, 72, 10]. Similarly, the forecast meteorological data, augmented with the same static features, formed a segment with nine features shaped [batch size, 120, 9]. Integrating these segments into a unified input sequence required aligning both the time and feature dimensions. To handle the feature dimension mismatch for the future segment (lacking future discharge), different strategies were employed based on prior work. Zero-padding was used for the missing feature dimension for the LSTM, GRU, and Seq2Seq models, consistent with benchmark implementations (Demir et al., 2022). For the Transformer model, the persistence method (repeating the last known discharge value) was applied, following Demiray et al. (2024). A similar persistence approach was adopted for the Mamba model in this study.

With the feature dimension aligned to ten for both historical and future segments using these strategies, the segments were concatenated along the time dimension. This resulted in a final unified input tensor with dimensions [batch size, 192, 10] which was fed into the LSTM, GRU, Transformer, and Mamba models. With the experimental setup and input data preparation clarified, the following analysis focuses on evaluating model performance across the diverse set of 125 individual sensor locations within Iowa. Assessing performance on a location-by-location basis is crucial for understanding the models' generalizability and robustness across different hydrological regimes and catchment characteristics present in the study region.

To synthesize the performance across these numerous locations into a concise summary, we first calculated the primary performance metrics for each model at each of the 125 stations individually. Specifically, for metrics like NSE, KGE, and Pearson's r, the median score over the 120-hour forecast horizon was determined for each station. For NRMSE, the overall error across the entire 120-hour period was calculated per station. Subsequently, to represent the typical performance across the entire set of locations while mitigating the influence of potential outliers at specific sites, the median value of these 125 station-specific scores was computed for each metric.

Table 3 presents these aggregate median performance scores, offering a comprehensive overview of how each model typically performed across the diverse geographical and hydrological conditions represented by the 125 stations. An initial observation is that all deep learning models substantially outperform the Persistence baseline across every metric, underscoring their advanced capabilities in capturing complex hydrological dynamics.

Focusing on the more sophisticated architectures, both the Transformer and Mamba models demonstrate superior performance compared to the LSTM, GRU, and Seq2Seq models. In terms of the Normalized Root Mean Square Error (NRMSE), which indicates relative prediction error,

both Transformer and Mamba yield the lowest median values, with Mamba showing a further reduction in error. This suggests higher overall accuracy for these two models.

Table 3. Aggregate median performance of models across 125 sensor locations for 120-hour hourly streamflow prediction (↑ higher is better, ↓ lower is better).

Method	**NSE ↑**	**KGE ↑**	**R ↑**	**NRMSE ↓**
Persistence	0.2147	0.6098	0.6340	1.0652
Seq2Seq	0.6675	0.7257	0.8715	0.6871
GRU	0.6607	0.7489	0.8571	0.7064
LSTM	0.6555	0.7686	0.8733	0.7090
Transformer	0.7461	0.7917	0.8844	0.6340
Mamba	0.7749	0.8260	0.8926	0.5782

Similarly, for Pearson's r, which measures the linear correlation between predicted and observed values, both Mamba and Transformer achieve the highest median scores. This indicates their strong ability to capture the general trend of streamflow variations, with Mamba exhibiting a marginally stronger correlation. The Nash-Sutcliffe Efficiency (NSE) and Kling-Gupta Efficiency (KGE) provide more holistic evaluations of model fit. Here again, the Mamba and Transformer models lead the other deep learning approaches. Both achieve the highest median NSE and KGE scores, reflecting better overall agreement with observed data and a good balance of correlation, bias, and variability representation. While both are strong, Mamba demonstrates a lead in these median scores as well.

These results suggest that both Transformer and Mamba architectures are highly effective for the generalized 120-hour hourly forecasting task. The Mamba model, in particular, shows performance that is comparable to, and in these aggregate median terms, slightly better than the Transformer model, positioning it as a compelling alternative for this type of hydrological application. The LSTM, GRU, and Seq2Seq models, while capable, generally do not reach the same level of median performance as the Transformer and Mamba architectures in this comparative setting.

To further investigate the temporal stability and typical performance of the models across the forecast horizon, the hourly Nash-Sutcliffe Efficiency (NSE) and Kling-Gupta Efficiency (KGE) scores were analyzed. For each hour of the 120-hour prediction window, the NSE and KGE were calculated for all 125 stations. The median of these 125 station-specific scores was then determined for that particular hour. This process yielded a time series of 120 hourly median NSE and KGE values for each model, representing the typical performance trend across the study locations as the forecast lead time increases. These hourly median performance trends are illustrated in Figures 2 and 3 for NSE and KGE values, respectively.

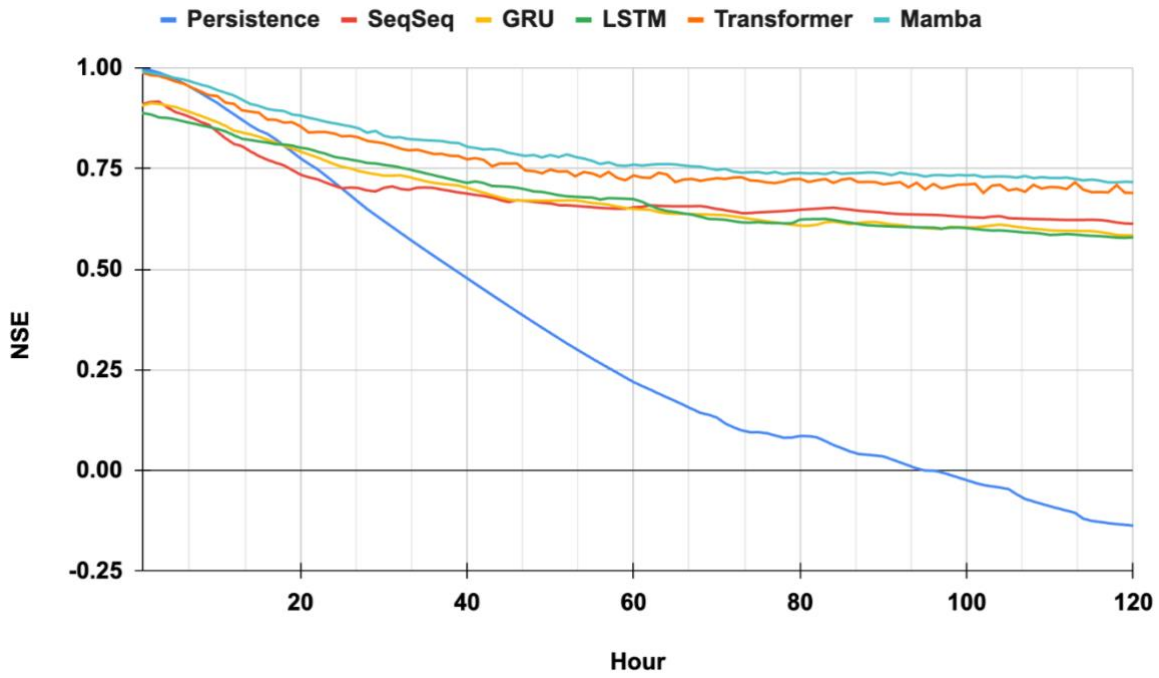

Figure 2. Hourly median NSE scores for 120-hour streamflow prediction across 125 stations.

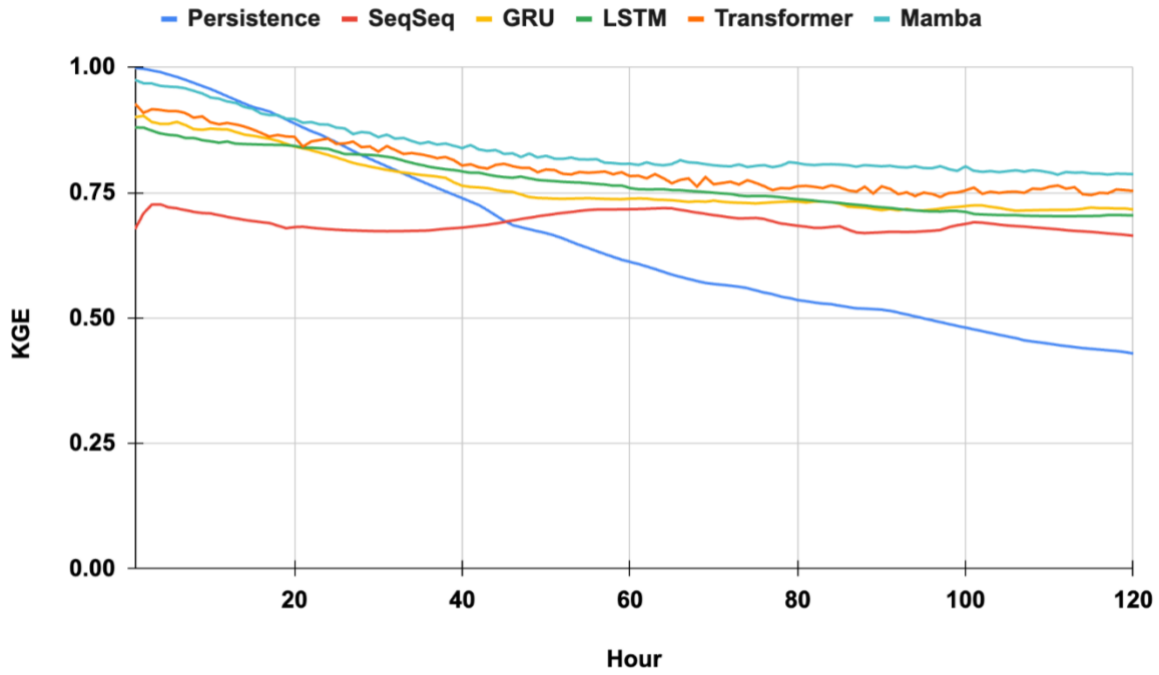

Figure 3. Hourly median KGE scores for 120-hour streamflow prediction across 125 stations.

Observing Figure 2, the hourly median NSE scores for all deep learning models generally start high and exhibit a gradual decline as the forecast horizon extends. The Persistence model's NSE, as expected, degrades much more rapidly, falling below zero typically after approximately 80-90 hours. Among the deep learning models, both Transformer and Mamba consistently

maintain higher median NSE values throughout the 120-hour period compared to LSTM, GRU, and Seq2Seq. Mamba shows a median NSE trajectory that is closely comparable to, and often slightly above, that of the Transformer, particularly in the later forecast hours, suggesting a robust typical performance over longer lead times. The LSTM, GRU, and Seq2Seq models perform similarly to each other, generally maintaining positive median NSE values for the entire duration but at a lower level than Transformer and Mamba.

A similar pattern is evident in Figure 3, which displays the hourly median KGE scores. Again, Transformer and Mamba exhibit the highest median KGE values across most of the forecast horizon, indicating a better overall agreement in terms of correlation, bias, and variability compared to the other models. Mamba's median KGE performance appears marginally better or highly competitive with the Transformer model throughout the 120 hours. The LSTM and GRU models also demonstrate relatively stable and positive median KGE scores, typically outperforming Seq2Seq in this metric, while all deep learning models significantly surpass the rapidly declining KGE of the Persistence model.

To summarize the characteristics of these 120 hourly median NSE and KGE time series for each model, Table 4 and Table 5 present their statistical distributions, including the maximum, minimum, median, and mean values.

Table 4. Statistical summary of the 120 hourly median NSE values presented in Figure 2.

	Max	**Min**	**Median**	**Mean**
Persistence	0.99867	-0.13669	0.21524	0.32133
SeqSeq	0.91700	0.61375	0.65652	0.68604
GRU	0.91327	0.58458	0.64956	0.68456
LSTM	0.88852	0.57870	0.67096	0.68684
Transformer	0.98900	0.69023	0.72987	0.76977
Mamba	0.99227	0.71627	0.76076	0.79489

Table 5. Statistical summary of the 120 hourly median KGE values presented in Figure 3.

	Max	**Min**	**Median**	**Mean**
Persistence	0.99890	0.42959	0.60987	0.65910
SeqSeq	0.72668	0.66427	0.68447	0.69010
GRU	0.90335	0.71388	0.73754	0.76524
LSTM	0.87996	0.70296	0.75803	0.77068
Transformer	0.92704	0.74148	0.78505	0.80011
Mamba	0.97491	0.78595	0.80991	0.83707

The statistics in Table 4 and Table 5 further reinforce the observations from the figures. For NSE (Table 4), Mamba achieves the highest mean and median of the hourly median NSE scores, and its minimum hourly median NSE remains substantially higher than those of LSTM, GRU, and Seq2Seq, closely matching the Transformer's minimum. This indicates that Mamba's typical performance, even at its weakest hour across the median of stations, is robust. The Transformer also shows strong statistics, with its median and mean hourly median NSE being second only to Mamba.

Similarly, for KGE (Table 5), Mamba leads in the mean and median of the hourly median KGE scores. Notably, Mamba's minimum hourly median KGE is the highest among all models, suggesting that its typical KGE performance across stations does not degrade as much as other models over the forecast horizon. The Transformer again presents strong results, with the second-highest mean and median, and the second-highest minimum hourly median KGE. These tables underscore the consistent and high-level typical performance of both Mamba and Transformer over the entire 120-hour prediction window compared to the other baselines.

To provide a more direct comparison of model superiority at individual locations, a head-to-head analysis was conducted. For each of the 125 stations, the primary performance metrics (median NSE, KGE, and Pearson's r over the 120-hour forecast, and overall NRMSE for the 120-hour period) were compared pairwise between all models. Tables 6 and 7 summarize these comparisons, indicating the number of stations (out of 125) where the row model outperformed the column model for the specified metrics.

Table 6. Head-to-Head Model Comparison Across 125 Stations Based on Median NSE / KGE Scores

Methods	**Persistence**		**Seq2Seq**		**GRU**		**LSTM**		**Transformer**		**Mamba**	
	NSE	**KGE**	**NSE**	**KGE**	**NSE**	**KGE**	**NSE**	**KGE**	**NSE**	**KGE**	**NSE**	**KGE**
Persistence	0	0	46	84	34	54	37	52	21	35	17	26
Seq2Seq	79	41	0	0	63	35	59	35	38	21	32	19
GRU	91	71	62	90	0	0	65	59	40	34	36	28
LSTM	88	73	66	90	60	66	0	0	41	54	33	43
Transformer	104	90	87	104	85	91	84	71	0	0	49	49
Mamba	108	99	93	106	89	97	92	82	76	76	0	0

Table 6 details the pairwise comparisons based on median NSE and KGE scores across the 125 stations. As expected, all deep learning models demonstrate a significant advantage over the Persistence baseline, outperforming it in the majority of locations for both NSE and KGE. When comparing the more advanced architectures, Mamba and Transformer both consistently outperform LSTM, GRU, and Seq2Seq in a large number of station-wise comparisons. In the direct head-to-head contest between Mamba and Transformer, the results show that Mamba

achieved a higher median NSE in 76 stations, compared to 49 stations where Transformer performed better. For median KGE, Mamba also outperformed Transformer in 76 stations, again versus 49 stations for the Transformer. These figures indicate a clear advantage for Mamba in terms of station-wise wins for these overall model fit metrics when compared directly against the Transformer.

Table 7. Head-to-Head Model Comparison Across 125 Stations Based on NRMSE / Pearson's r Scores

Methods	Persistence		Seq2Seq		GRU		LSTM		Transformer		Mamba	
	NSE	KGE	NSE	KGE	NSE	KGE	NSE	KGE	NSE	KGE	NSE	KGE
Persistence	0	0	44	12	34	21	35	20	16	10	16	14
Seq2Seq	81	113	0	0	63	75	62	73	32	56	28	51
GRU	91	104	62	50	0	0	66	56	37	40	28	38
LSTM	90	105	63	52	59	69	0	0	37	47	32	45
Transformer	109	115	93	69	88	85	88	78	0	0	46	51
Mamba	109	111	97	74	97	87	93	80	79	74	0	0

Table 7 presents similar head-to-head comparisons using NRMSE (where a lower value signifies better performance) and Pearson's r (where a higher value is better). The general outperformance of deep learning models over Persistence is again evident. Focusing on the Mamba versus Transformer comparison, Mamba achieved a better (lower) NRMSE in 79 stations, while Transformer had a lower NRMSE in 46 stations. For Pearson's r, Mamba demonstrated a higher correlation coefficient in 74 stations, compared to 51 stations where Transformer was superior. These pairwise counts, particularly for NRMSE and Pearson's r, further underscore Mamba's strong station-wise performance, often achieving better error magnitudes and linear trend representation than the Transformer.

Overall, the detailed head-to-head comparisons presented in Tables 6 and 7 reinforce the findings from the aggregate metrics, suggesting that both Mamba and Transformer are the leading architectures. However, these station-wise win counts indicate that the Mamba model consistently outperformed the Transformer model across a majority of the 125 locations for all four metrics evaluated (NSE, KGE, NRMSE, and Pearson's r). This robust station-level performance positions Mamba as a highly effective and often superior alternative to the Transformer for this generalized long-horizon streamflow forecasting task.

In summary, the comprehensive performance evaluation across 125 diverse locations in Iowa demonstrates that while all deep learning models significantly surpassed the Persistence baseline, the Mamba and Transformer architectures consistently emerged as the leading performers for the 120-hour hourly streamflow forecasting task. The analysis of aggregate median metrics and hourly performance trends highlighted both models as superior to other deep learning

approaches. Crucially, the station-by-station head-to-head comparisons (Tables 6 and 7) revealed that the Mamba model generally outperformed the Transformer model across a majority of individual locations for all four-evaluation metrics (NSE, KGE, NRMSE, and Pearson's r). This robust and often superior station-level performance positions Mamba not just as a compelling alternative, but as a potentially more effective architecture for generalized long-horizon streamflow prediction within the context of this study. While LSTM, GRU, and Seq2Seq models provided reasonable predictions, they typically did not match the higher performance levels achieved by Mamba and Transformer in this extensive evaluation.

While these quantitative metrics are crucial for assessing predictive accuracy and reliability, a deeper understanding of how these complex models arrive at their predictions is essential for building trust, gaining scientific insights, and ensuring responsible application in critical areas like water resource management. Therefore, the following subsection delves into an interpretability analysis using Explainable AI (XAI) techniques to shed light on the inner workings of the tested models.

4.3. Explainable AI Investigation

To gain deeper insights into the decision-making process of the top-performing models, Mamba and Transformer, and to understand how they utilize input features to generate streamflow forecasts, this study employs Explainable AI (XAI) techniques. Given the complexity of these advanced deep learning architectures, methods that can provide transparency into model behavior are invaluable for validating model learning, identifying influential factors, and increasing user trust in hydrological applications.

In this work, we utilize SHapley Additive exPlanations (SHAP) (Lundberg & Lee, 2017), a game theory-based approach that has become a prominent method for explaining the output of any machine learning model. SHAP values explain the prediction of an instance by computing the contribution of each feature to the prediction. For a given prediction, the SHAP value for a feature represents how much that feature's value contributed to pushing the model's output away from the baseline (average) prediction. This method allows for an assessment of both overall feature importance across the dataset and the impact of features on individual predictions. SHAP values were computed for a representative subset of the test data for the Mamba, Transformer, LSTM, and GRU models. The overall importance of each input feature for the Mamba, Transformer, LSTM, and GRU models is illustrated by their respective mean absolute SHAP values, presented in Figures 4, and 5. These plots rank features based on their average impact magnitude on the model output.

Examining the feature importance for the Mamba and Transformer models (Figure 4), both architectures show a consensus on the primary drivers of streamflow prediction. For both models, 'Streamflow' (representing lagged observations) is unequivocally the most influential predictor, followed in identical order by 'Precipitation', 'Area', 'Travel Time', and 'Silt' as the next four most important features. This strong agreement on the top five features underscores their fundamental role in the hydrological processes captured by these diverse architectures. While the

ranking of these leading features is consistent, their mean absolute SHAP values (Figure 4) indicate some differences in the magnitude of their influence. The Transformer model assigns a higher average impact to 'Streamflow' and a slightly greater impact to 'Precipitation' compared to Mamba. Conversely, Mamba attributes a higher relative importance to 'Travel Time' and 'Silt' than the Transformer. For 'Area', both models show very similar magnitudes of importance. Beyond these top five, the precise ranking and relative importance of other features, such as the various soil types and 'Evapotranspiration', show further variations, suggesting subtle differences in how each model incorporates more secondary information after accounting for the primary drivers.

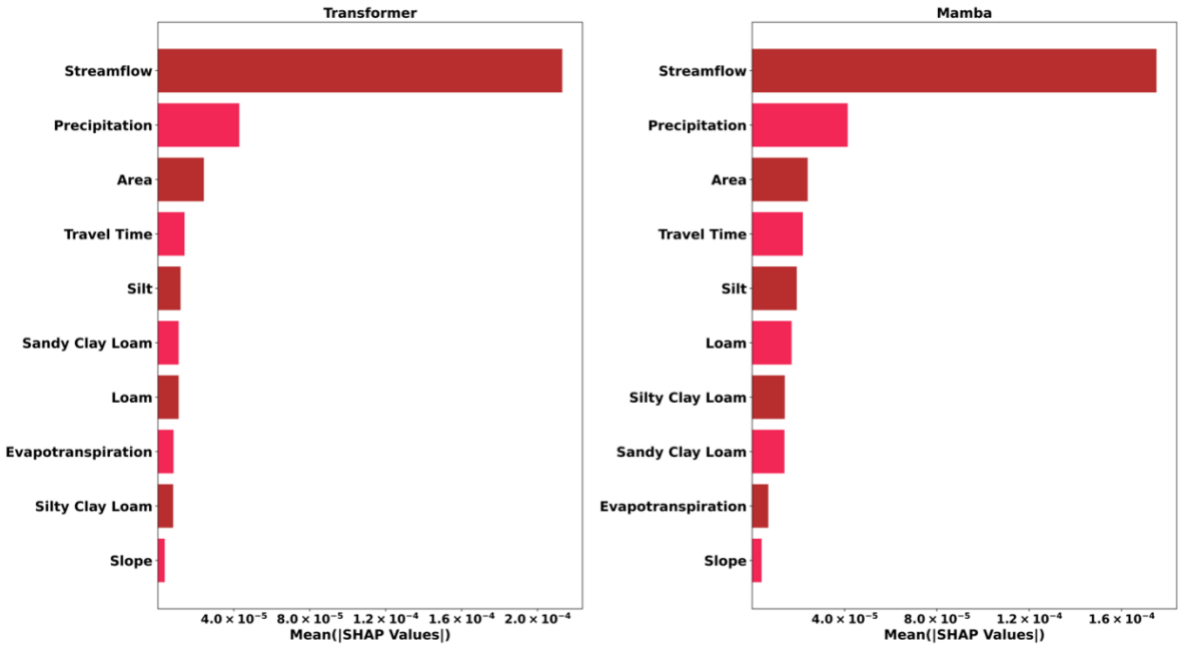

Figure 4. Global feature importance for the Transformer and Mamba models, showing mean absolute SHAP values.

Turning to the RNN-based architectures, the LSTM and GRU models (Figure 5) also identify 'Streamflow' as the unequivocally most important feature, mirroring the findings from Mamba and Transformer. Following 'Streamflow', both LSTM and GRU rank 'Area' as their second most influential input. Beyond this, their feature prioritization shows some variation. For the GRU model, 'Travel Time' emerges as the third most significant feature, followed by 'Precipitation', with soil characteristics such as 'Sandy Clay Loam' and 'Loam' having a more moderate impact. In contrast, the LSTM model gives higher importance to soil types 'Silt' and 'Loam' (ranking third and fourth respectively) after 'Area', with 'Travel Time' and 'Precipitation' following these. This indicates that while both LSTM and GRU leverage recent streamflow and catchment area strongly, they differ in their subsequent reliance on routing parameters versus specific soil types or direct precipitation inputs. The overall magnitudes of mean SHAP values for most secondary

features in LSTM and GRU are generally somewhat lower than those observed for the top secondary features in Mamba and Transformer.

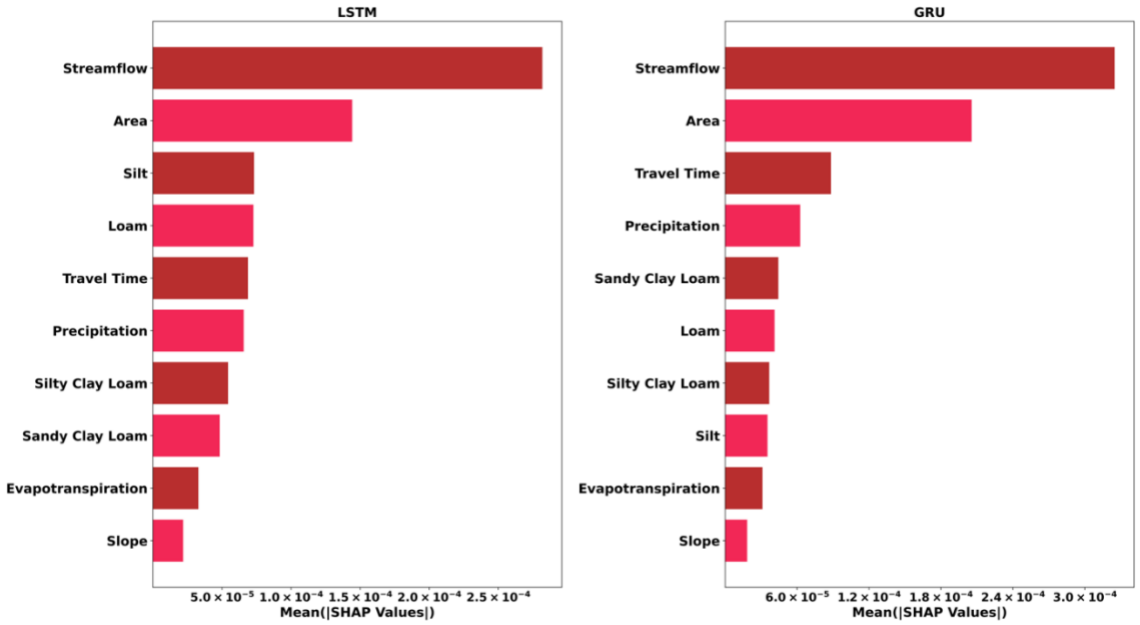

Figure 5. Global feature importance for the LSTM and GRU models, showing mean absolute SHAP values.

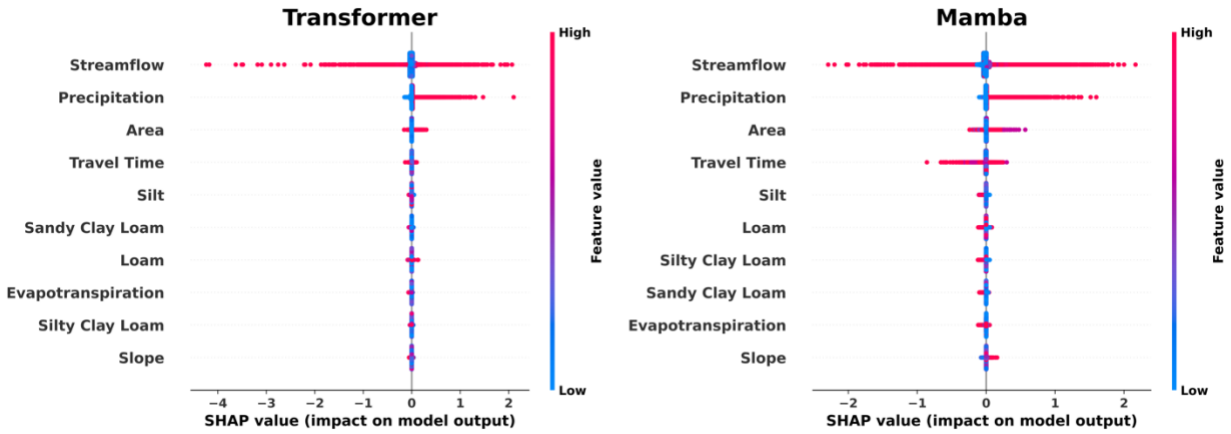

Figure 6. SHAP summary plot for the Transformer and Mamba models, illustrating the distribution of SHAP values for each input feature.

To understand not just the magnitude but also the direction and consistency of feature impacts, SHAP summary plots (often referred to as bee-swarm plots) are presented in Figures 6 (Transformer and Mamba), and 7 (LSTM and GRU). These plots display the distribution of SHAP values for each feature across all explained instances, with color typically indicating the original value of the feature (high or low).

Figure 6 displays the SHAP summary plots for the Mamba and Transformer models, highlighting the relative influence of input features on model predictions. In both models, previous streamflow emerges as the dominant driver of predictive output, with consistently high SHAP values across the dataset. Precipitation ranks second, showing positive SHAP contributions, particularly at higher magnitudes (as indicated by red-colored points on the right-hand side). While both models leverage station-based descriptors such as area and travel time, the Mamba model shows a slightly broader distribution of SHAP values for these features, suggesting stronger sensitivity to basin-scale variability. The Transformer model, on the other hand, shows more compact SHAP distributions, especially for soil texture features, indicating a more uniform treatment of static spatial attributes. Notably, Mamba appears to better integrate both static and dynamic hydrological inputs, possibly due to its selective state-space mechanism, which adaptively modulates feature importance across time. This may explain the greater variance in SHAP values for static features in Mamba relative to Transformer.

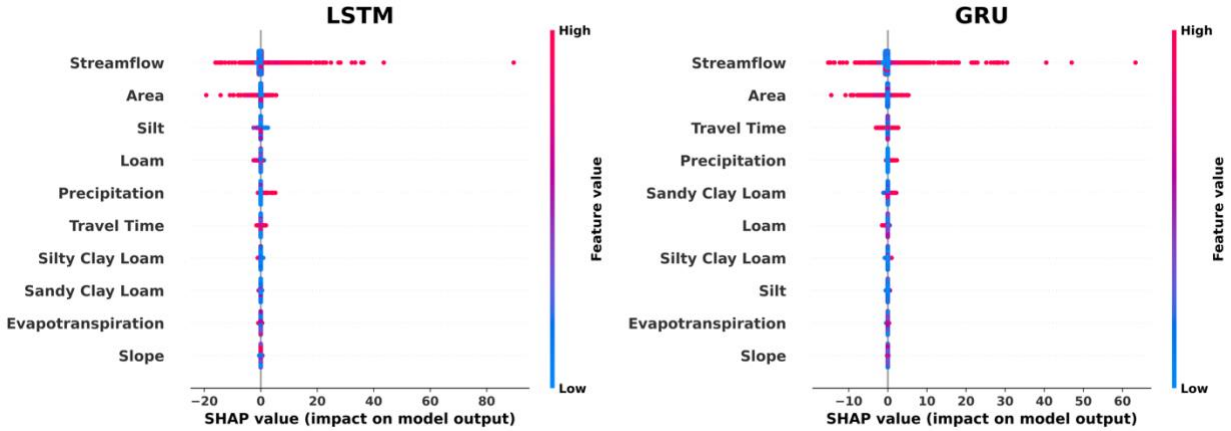

Figure 7. SHAP summary plot for the LSTM and GRU models, illustrating the distribution of SHAP values for each input feature.

Figure 7 shows the SHAP summary plots for the LSTM and GRU models. In both models, previous streamflow dominates feature importance, followed by area, which likely captures differences in basin size and hydrological response times. Compared to Mamba and Transformer, the LSTM and GRU models exhibit narrower SHAP distributions and more uniform feature impacts, indicating more stable but less dynamic sensitivity to varying input values. The GRU model, in particular, shows slightly more dispersion in SHAP values for travel time and precipitation, yet still reflects a relatively consistent reliance on temporal features. Both models assign considerably lower importance to soil texture features and evapotranspiration, suggesting that their sequential architecture may limit the incorporation of static spatial characteristics.

Synthesizing the XAI findings across the Mamba, Transformer, LSTM, and GRU models (Figures 4-7) reveals that while lagged 'Streamflow' is universally the most dominant predictive feature—reflecting its critical role in capturing the autoregressive nature of hydrological systems—the models diverge in their subsequent utilization of other inputs. 'Precipitation', a

primary driver of runoff generation, consistently shows a positive impact on predicted streamflow when its values are high. This effect appears particularly direct and strong for the Mamba and Transformer models, where 'Precipitation' ranks as the second most important feature globally.

In contrast, for LSTM and GRU, while still influential, 'Precipitation' often ranks after static catchment characteristics, suggesting these RNN-based models might integrate its signal differently. The static feature 'Area' is recognized as highly important by all models, generally contributing positively to predictions; this aligns with the hydrological principle that larger catchments typically yield greater runoff volumes. Notably, for LSTM and GRU, 'Area' is the second most crucial feature after 'Streamflow', underscoring its significance for these architectures. 'Travel Time', which represents the time taken for water to concentrate, showed varied importance; the Mamba model uniquely demonstrated that higher 'Travel Time' values often exerted a negative influence on its predictions, potentially capturing how longer concentration times can attenuate flood peaks or delay runoff response.

For the Transformer, LSTM, and GRU, 'Travel Time' generally exhibited a less consistently directional or less impactful role based on individual predictions. Other static features like soil types and slope, while contributing, generally showed more modest and conditional impacts across all models, indicating their influence is likely secondary to the primary dynamic drivers and broad catchment descriptors. These XAI-derived insights, by linking feature impacts to hydrological understanding, are crucial for building confidence and discerning the nuanced ways these complex models learn to forecast streamflow.

In essence, the comprehensive evaluation presented in this section highlights the Mamba architecture as a highly effective approach for 120-hour hourly generalized streamflow forecasting. Quantitative performance metrics indicated that Mamba not only significantly surpassed conventional deep learning models like LSTM, GRU, Seq2Seq, and the Persistence baseline, but also generally outperformed the strong Transformer model across a majority of the 125 diverse locations when evaluated on a station-by-station basis for all key metrics.

The subsequent Explainable AI analysis further illuminated the decision-making processes of these models, revealing that while all architectures learned hydrologically relevant dependencies, particularly on recent streamflow, they exhibited distinct patterns in their utilization of secondary dynamic and static features. These combined findings—demonstrating Mamba's robust predictive skill and providing interpretable insights into its operational behavior—underscore its considerable potential as an advanced tool for complex, long-horizon hydrological forecasting tasks. The broader implications of these results and avenues for future research will be discussed in the concluding section.

5. Conclusions

This study undertook a comprehensive evaluation of Mamba architecture, a novel deep learning model based on State Space Models, for the challenging task of generalized, 120-hour hourly streamflow forecasting across 125 diverse locations in Iowa, USA. The primary objectives were

to assess Mamba's predictive performance against established baseline models—including Persistence, LSTM, GRU, Seq2Seq, and the Transformer—and to leverage Explainable AI (XAI) techniques, specifically SHAP analysis, to interpret the Mamba model's decision-making process and compare its feature utilization with that of the Transformer.

The experimental results demonstrated that Mamba architecture achieves a high level of predictive accuracy. Across various aggregate median performance metrics (NSE, KGE, Pearson's r, and NRMSE), Mamba consistently ranked as the top-performing model. More notably, detailed station-by-station head-to-head comparisons revealed that Mamba generally outperformed the Transformer baseline across a majority of individual locations for all four-evaluation metrics. Both Mamba and Transformer significantly surpassed the Persistence method and other deep learning architectures like LSTM, GRU, and Seq2Seq. The analysis of hourly performance trends further indicated Mamba's robustness in maintaining predictive skill over the extended 120-hour forecast horizon. Furthermore, the XAI analysis provided valuable insights into the feature importance and impact patterns learned by Mamba, Transformer, LSTM, and GRU, revealing distinct strategies in their reliance on dynamic meteorological inputs versus static catchment characteristics, while confirming that the models generally learned hydrologically sound relationships.

The principal contributions of this research include the rigorous evaluation of the recent Mamba architecture in a large-scale, generalized hydrological forecasting context and the demonstration of its potential as an efficient and effective alternative to attention-based models for long-horizon predictions. The integration of XAI not only enhances the transparency of the Mamba model but also offers a pathway to better understand and trust complex deep learning predictions in critical water resource management and flood forecasting applications. The findings suggest that Mamba's unique architecture, which combines linear-time complexity with effective long-range dependency modeling, holds a significant promise for advancing the field of hydrological forecasting.

While this study provides strong evidence for Mamba's capabilities, certain limitations should be acknowledged. The evaluation was conducted on catchments within a specific geographical region (Iowa, USA), and further research is needed to assess its performance in more diverse hydro-climatic settings. Additionally, while a standard Mamba configuration was explored, an exhaustive hyperparameter optimization or investigation into various Mamba architectural variants was beyond the scope of this work. The XAI analysis, though insightful, focused on SHAP values, and other interpretability methods might reveal different facets of model behavior.

Future research should aim to explore Mamba architecture's scalability and performance on even larger and more varied hydrological datasets. Investigating different Mamba configurations, including their potential in hybrid models, could yield further improvements. Applying Mamba to other hydrological prediction tasks, such as flood inundation mapping or water quality forecasting, would also be valuable. Continued exploration of XAI techniques will be crucial for further demystifying these advanced models and fostering their adoption in operational

hydrological forecasting systems, potentially leading to more timely and accurate information for disaster preparedness and sustainable water management.

6. References

Ahmed, A.M., Deo, R.C., Feng, Q., Ghahramani, A., Raj, N., Yin, Z. and Yang, L., 2021. Deep learning hybrid model with Boruta-Random forest optimiser algorithm for streamflow forecasting with climate mode indices, rainfall, and periodicity. Journal of Hydrology, 599, p.126350.

Alabbad, Y., Yildirim, E., & Demir, I., 2023. A web-based analytical urban flood damage and loss estimation framework. Environmental Modelling & Software, 163, 105670.

Alabbad, Y., Mount, J., Campbell, A.M. and Demir, I., 2024. A web-based decision support framework for optimizing road network accessibility and emergency facility allocation during flooding. *Urban Informatics*, *3*(1), p.10.

Arnold, J.G., Williams, J.R., Srinivasan, R., King, K.W. and Griggs, R.H., 1994. SWAT: Soil and water assessment tool. US Department of Agriculture, Agricultural Research Service, Grassland, Soil and Water Research Laboratory, Temple, TX, 494.

Arnold, J.G., Moriasi, D.N., Gassman, P.W., Abbaspour, K.C., White, M.J., Srinivasan, R., Santhi, C., Harmel, R.D., Van Griensven, A., Van Liew, M.W. and Kannan, N., 2012. SWAT: Model use, calibration, and validation. Transactions of the ASABE, 55(4), pp.1491-1508.

Bayar, S., Demir, I. and Engin, G.O., 2009. Modeling leaching behavior of solidified wastes using back-propagation neural networks. *Ecotoxicology and environmental safety*, *72*(3), pp.843-850.

Beven, K.J. and Kirkby, M.J., 1979. A physically based, variable contributing area model of basin hydrology/Un modèle à base physique de zone d'appel variable de l'hydrologie du bassin versant. Hydrological sciences journal, 24(1), pp.43-69.

Castangia, M., Grajales, L.M.M., Aliberti, A., Rossi, C., Macii, A., Macii, E. and Patti, E., 2023. Transformer neural networks for interpretable flood forecasting. Environmental Modelling & Software, 160, p.105581.

Cho, K., Van Merriënboer, B., Bahdanau, D. and Bengio, Y., 2014. On the properties of neural machine translation: Encoder-decoder approaches. *arXiv preprint arXiv:1409.1259*.

Cikmaz, B.A., Yildirim, E. and Demir, I., 2025. Flood susceptibility mapping using fuzzy analytical hierarchy process for Cedar Rapids, Iowa. *International journal of river basin management*, *23*(1), pp.1-13.

Davenport, F.V., Burke, M. and Diffenbaugh, N.S., 2021. Contribution of historical precipitation change to US flood damages. Proceedings of the National Academy of Sciences, 118(4), p.e2017524118.

Demir, I. and Szczepanek, R., 2017. Optimization of river network representation data models for web-based systems. *Earth and Space Science*, *4*(6), pp.336-347.

Demir, I., Xiang, Z., Demiray, B. and Sit, M., 2022. Waterbench: a large-scale benchmark dataset for data-driven streamflow forecasting. Earth System Science Data Discussions, 2022, pp.1-19.

Demiray, B.Z., Sit, M., Mermer, O. and Demir, I., 2024. Enhancing hydrological modeling with transformers: a case study for 24-h streamflow prediction. Water Science & Technology, 89(9), pp.2326-2341.

Demiray, B.Z. and Demir, I., 2024. Towards Generalized Hydrological Forecasting using Transformer Models for 120-Hour Streamflow Prediction. *arXiv preprint arXiv:2406.07484*.

Devia, G.K., Ganasri, B.P. and Dwarakish, G.S., 2015. A review on hydrological models. Aquatic procedia, 4, pp.1001-1007.

Eccles, R., Zhang, H., Hamilton, D., Trancoso, R. and Syktus, J., 2021. Impacts of climate change on streamflow and floodplain inundation in a coastal subtropical catchment. Advances in Water Resources, 147, p.103825.

Ewing, G., Mantilla, R., Krajewski, W. and Demir, I., 2022. Interactive hydrological modelling and simulation on client-side web systems: an educational case study. *Journal of Hydroinformatics*, *24*(6), pp.1194-1206.

Fang, J., Yang, L., Wen, X., Yu, H., Li, W., Adamowski, J.F. and Barzegar, R., 2024. Ensemble learning using multivariate variational mode decomposition based on the transformer for multi-step-ahead streamflow forecasting. *Journal of Hydrology*, *636*, p.131275.

Feng, D., Fang, K. and Shen, C., 2020. Enhancing streamflow forecast and extracting insights using long-short term memory networks with data integration at continental scales. *Water Resources Research*, *56*(9), p.e2019WR026793.

Goodfellow, I., Bengio, Y., Courville, A. and Bengio, Y., 2016. *Deep learning* (Vol. 1, No. 2). Cambridge: MIT press.

Granata, F., Gargano, R. and De Marinis, G., 2016. Support vector regression for rainfall-runoff modeling in urban drainage: A comparison with the EPA's storm water management model. Water, 8(3), p.69.

Gu, A., Goel, K. and Ré, C., 2021. Efficiently modeling long sequences with structured state spaces. *arXiv preprint arXiv:2111.00396*.

Gu, A. and Dao, T., 2023. Mamba: Linear-time sequence modeling with selective state spaces. arXiv preprint arXiv:2312.00752.

Guo, Y., Xu, Y.P., Yu, X., Chen, H., Gu, H. and Xie, J., 2020. AI-based techniques for multi-step streamflow forecasts: application for multi-objective reservoir operation optimization and performance assessment. Hydrology and Earth System Sciences Discussions, 2020, pp.1-52.

Gupta, H.V., Kling, H., Yilmaz, K.K. and Martinez, G.F., 2009. Decomposition of the mean squared error and NSE performance criteria: Implications for improving hydrological modelling. *Journal of hydrology*, *377*(1-2), pp.80-91.

He, M., Jiang, S., Ren, L., Cui, H., Qin, T., Du, S., Zhu, Y., Fang, X. and Xu, C.Y., 2024. Streamflow prediction in ungauged catchments through use of catchment classification and deep learning. Journal of Hydrology, 639, p.131638.

Hochreiter, S. and Schmidhuber, J., 1997. Long short-term memory. *Neural computation*, *9*(8), pp.1735-1780.

Honorato, A.G.D.S.M., Silva, G.B.L.D. and Guimaraes Santos, C.A., 2018. Monthly streamflow forecasting using neuro-wavelet techniques and input analysis. Hydrological Sciences Journal, 63(15-16), pp.2060-2075.

Hou, H., Huang, Z., Tan, K., Lu, R. and Yu, F.R., 2025. RWKV-X: A Linear Complexity Hybrid Language Model. arXiv preprint arXiv:2504.21463.

Ibrahim, K.S.M.H., Huang, Y.F., Ahmed, A.N., Koo, C.H. and El-Shafie, A., 2022. A review of the hybrid artificial intelligence and optimization modelling of hydrological streamflow forecasting. *Alexandria Engineering Journal*, *61*(1), pp.279-303.

IPCC, 2023: Sections. In: Climate Change 2023: Synthesis Report. Contribution of Working Groups I, II and III to the Sixth Assessment Report of the Intergovernmental Panel on Climate Change [Core Writing Team, H. Lee and J. Romero (eds.)]. IPCC, Geneva, Switzerland, pp. 35-115, doi: 10.59327/IPCC/AR6-9789291691647.

Jhong, Y.D., Chen, C.S., Jhong, B.C., Tsai, C.H. and Yang, S.Y., 2024. Optimization of LSTM parameters for flash flood forecasting using genetic algorithm. *Water Resources Management*, *38*(3), pp.1141-1164.

Jia, D., Li, W., Huang, D. and Chen, S., 2024. Daily runoff prediction based on lightweight Mamba with partial normalization. Hydrology Research, 55(12), pp.1182-1196.

Khan, S., Naseer, M., Hayat, M., Zamir, S.W., Khan, F.S. and Shah, M., 2022. Transformers in vision: A survey. *ACM computing surveys (CSUR)*, *54*(10s), pp.1-41.

Kling, H., Fuchs, M. and Paulin, M., 2012. Runoff conditions in the upper Danube basin under an ensemble of climate change scenarios. *Journal of hydrology*, *424*, pp.264-277.

Koya, S.R. and Roy, T., 2024. Temporal fusion transformers for streamflow prediction: Value of combining attention with recurrence. *Journal of Hydrology*, *637*, p.131301.

Krajewski, W.F., Ghimire, G.R., Demir, I. and Mantilla, R., 2021. Real-time streamflow forecasting: AI vs. Hydrologic insights. *Journal of Hydrology X*, *13*, p.100110.

Kratzert, F., Klotz, D., Brenner, C., Schulz, K. and Herrnegger, M., 2018. Rainfall–runoff modelling using long short-term memory (LSTM) networks. Hydrology and Earth System Sciences, 22(11), pp.6005-6022.

Krause, P., Boyle, D.P. and Bäse, F., 2005. Comparison of different efficiency criteria for hydrological model assessment. *Advances in geosciences*, *5*, pp.89-97.

Lin, T., Wang, Y., Liu, X. and Qiu, X., 2022. A survey of transformers. AI open, 3, pp.111-132.

Liu, C., Liu, D. and Mu, L., 2022. Improved transformer model for enhanced monthly streamflow predictions of the Yangtze River. Ieee Access, 10, pp.58240-58253.

Lundberg, S.M. and Lee, S.I., 2017. A unified approach to interpreting model predictions. Advances in neural information processing systems, 30.

Luppichini, M., Barsanti, M., Giannecchini, R. and Bini, M., 2022. Deep learning models to predict flood events in fast-flowing watersheds. *Science of the total environment*, *813*, p.151885.

Ma, K., He, D., Liu, S., Ji, X., Li, Y. and Jiang, H., 2024. Novel time-lag informed deep learning framework for enhanced streamflow prediction and flood early warning in large-scale catchments. *Journal of Hydrology*, *631*, p.130841.

Mankari, S. and Sanghavi, A., 2025, March. Predicting Space Debris Rotation Using the Debris Rotation Prediction Network (DRPN). In *2025 International Conference on Next Generation Information System Engineering (NGISE)* (Vol. 1, pp. 1-6). IEEE.

Moreno-Pino, F., Arroyo, Á., Waldon, H., Dong, X. and Cartea, Á., 2024. Rough transformers: Lightweight and continuous time series modelling through signature patching. Advances in Neural Information Processing Systems, 37, pp.106264-106294.

Mosavi, A., Ozturk, P. and Chau, K.W., 2018. Flood prediction using machine learning models: Literature review. Water, 10(11), p.1536.

Mucllari, E., Daniels, Z., Zhang, D. and Ye, Q., 2025. Compact Recurrent Transformer with Persistent Memory. arXiv preprint arXiv:2505.00929.

Nash, J.E. and Sutcliffe, J.V., 1970. River flow forecasting through conceptual models part I—A discussion of principles. *Journal of hydrology*, *10*(3), pp.282-290.

Ng, K.W., Huang, Y.F., Koo, C.H., Chong, K.L., El-Shafie, A. and Ahmed, A.N., 2023. A review of hybrid deep learning applications for streamflow forecasting. Journal of Hydrology, 625, p.130141.

NOAA National Centers for Environmental Information (NCEI), 2022. US billion-dollar weather and climate disasters. https://www.ncei.noaa.gov/access/monitoring/billions/, DOI:10.25921/stkw-7w73.

Ren-Jun, Z., 1992. The Xinanjiang model applied in China. Journal of hydrology, 135(1-4), pp.371-381.

Reichstein, M., Camps-Valls, G., Stevens, B., Jung, M., Denzler, J., Carvalhais, N. and Prabhat, F., 2019. Deep learning and process understanding for data-driven Earth system science. *Nature*, *566*(7743), pp.195-204.

Sabzipour, B., Arsenault, R., Troin, M., Martel, J.L., Brissette, F., Brunet, F. and Mai, J., 2023. Comparing a long short-term memory (LSTM) neural network with a physically-based hydrological model for streamflow forecasting over a Canadian catchment. *Journal of Hydrology*, *627*, p.130380.

Sarker, I.H., 2021. Deep learning: a comprehensive overview on techniques, taxonomy, applications and research directions. *SN computer science*, *2*(6), pp.1-20.

Sharma, P. and Machiwal, D. eds., 2021. Advances in streamflow forecasting: from traditional to modern approaches. Elsevier.

Sit, M., Seo, B.C. and Demir, I., 2021. Iowarain: A statewide rain event dataset based on weather radars and quantitative precipitation estimation. *arXiv preprint arXiv:2107.03432*.

Sit, M., Demiray, B.Z. and Demir, I., 2022. A systematic review of deep learning applications in streamflow data augmentation and forecasting. EarthArxiv, 3617. https://doi.org/10.31223/X5HM08

Tabari, H., 2020. Climate change impact on flood and extreme precipitation increases with water availability. Scientific reports, 10(1), p.13768.

Tanir, T., Yildirim, E., Ferreira, C.M. and Demir, I., 2024. Social vulnerability and climate risk assessment for agricultural communities in the United States. *Science of The Total Environment*, *908*, p.168346.

Tripathy, K.P. and Mishra, A.K., 2024. Deep learning in hydrology and water resources disciplines: Concepts, methods, applications, and research directions. *Journal of Hydrology*, *628*, p.130458.

UNESCO, 2023. The United Nations world water development report 2023: partnerships and cooperation for water. UN. Available at: https://unesdoc.unesco.org/ark:/48223/pf0000384655.

Vaswani, A., Shazeer, N., Parmar, N., Uszkoreit, J., Jones, L., Gomez, A.N., Kaiser, Ł. and Polosukhin, I., 2017. Attention is all you need. Advances in neural information processing systems, 30.

Wen, Q., Zhou, T., Zhang, C., Chen, W., Ma, Z., Yan, J. and Sun, L., 2022. Transformers in time series: A survey. *arXiv preprint arXiv:2202.07125*.

Wilbrand, K., Taormina, R., ten Veldhuis, M.C., Visser, M., Hrachowitz, M., Nuttall, J. and Dahm, R., 2023. Predicting streamflow with LSTM networks using global datasets. *Frontiers in Water*, *5*, p.1166124.

World Meteorological Organization (WMO), 2021. The Atlas of Mortality and Economic Losses from Weather, Climate and Water Extremes (1970–2019). Available at: https://library.wmo.int/idurl/4/57564.

Wu, H., Xu, J., Wang, J. and Long, M., 2021. Autoformer: Decomposition transformers with auto-correlation for long-term series forecasting. *Advances in neural information processing systems*, *34*, pp.22419-22430.

Xiang, Z. and Demir, I., 2021. High-resolution rainfall-runoff modeling using graph neural network. arXiv preprint arXiv:2110.10833.

Xiang, Z. & Demir I. 2022. Real-Time Streamflow Forecasting Framework, Implementation and Post-analysis Using Deep Learning. EarthArxiv 3162. https://doi.org/10.31223/X5BW6R

Yaseen, Z.M., El-Shafie, A., Jaafar, O., Afan, H.A. and Sayl, K.N., 2015. Artificial intelligence based models for stream-flow forecasting: 2000–2015. Journal of Hydrology, 530, pp.829-844.

Yaseen, Z.M., Awadh, S.M., Sharafati, A. and Shahid, S., 2018. Complementary data-intelligence model for river flow simulation. Journal of Hydrology, 567, pp.180-190.

Zhang, Y., Zhou, Z., Van Griensven Thé, J., Yang, S.X. and Gharabaghi, B., 2023. Flood forecasting using hybrid LSTM and GRU models with lag Time Preprocessing. *Water*, *15*(22), p.3982.

Zhou, H., Zhang, S., Peng, J., Zhang, S., Li, J., Xiong, H. and Zhang, W., 2021, May. Informer: Beyond efficient transformer for long sequence time-series forecasting. In Proceedings of the AAAI conference on artificial intelligence (Vol. 35, No. 12, pp. 11106-11115).